

https://dspace.org/

# The development of Giant reed biochar for adsorption of Basic Blue 41 and Eriochrome Black T azo dyes from wastewater

**M Abdu; Saeideh Babaee; A Worku; T.A.M Msagati; Jemal Nure**

https://hdl.handle.net/10539/40382
WOS

Downloaded from a DSpace repository. https://dspace.org/

scientific reports

Check for updates

OPEN

# The development of Giant reed biochar for adsorption of Basic Blue 41 and Eriochrome Black T. azo dyes from wastewater

Mohammednur Abdu[1]✉, Saeideh Babaee[2], Abebe Worku[1], Titus A. M. Msagati[3] & Jemal Fito Nure[2]

**The textile industry is discharging high concentrations of anionic and cationic azo dyes into the nearby environment, which can cause adverse effects on public health, and the aquatic environment. Therefore, this study aimed to develop giant reed biochar and apply for the removal of Basic blue 41 (BB41) and Eriochrome black T (EBT) azo dyes from water. Characterization techniques such as BET surface area analyzer, Fourier-transform infrared spectroscopy (FT-IR), Raman spectroscopy, X-ray diffraction (XRD), scanning electron microscopy (SEM), and thermal gravimetric analyzer (TGA) were applied for biochar description. The biochar exhibits a high fixed carbon content (80.4%), a low ash content (3.8%), a large surface area (429.0 $m^2$/g), and good thermal stability. High removal efficiencies of BB41 98.6% and EBT 82.5% were recorded at the specific experimental condition. The experimental data were fitted with the Langmuir isotherm model at $R^2$ 0.99 for both dyes whereas the adsorption kinetics revealed the pseudo-second-order kinetics at $R^2 \sim 1$ and 0.99 for BB41 and EBT, respectively. Furthermore, four regenerations of biochar with adsorption performances of BB41 and EBT dyes were found to be 94.7% and 79.1%, respectively. Finally, this adsorbent can be considered an economically viable material for the removal of synthetic dyes from wastewater systems. In conclusion, the study findings showed that the adsorbent material is promising to apply for water and wastewater treatment but still, the study of adsorption interaction and modifications of the surface functionalities are essential to accommodate multipollutant removal from real water systems.**

**Keywords** Adsorbent, Biochar, Kinetics, Textile wastewater, Water pollution, Wastewater treatment

Water pollution is a global challenge that has been increasing worldwide, influencing economic growth and the physical ecosystem and public health of billions of people[1]. Global water scarcity is caused not only by resource scarcity but also by the progressive deterioration of water quality[2]. Poor water quality and inadequate wastewater management have led to severe water quality issues in many parts of the world. Human settlement activities, industries, and agriculture are the major sources of water pollution[3]. Industries are one of the major sources of water pollution, producing harmful pollutants to people and the environment. The textile industry is one of the most water-consuming and water quality deteriorating industrial sectors which is discharging a high amount of complex mixture of pollutants, such as dyes, metals, organic matter, and other pollutants[4,5]. Dye and pigments have been used for a long time for coloring goods in the textile, leather, cosmetics, as well as food industries. The textile industry uses several kinds of synthetic dyes for industrial operation but approximately 10–15% of these dyes end up in the wastewater during the manufacturing processing of textiles. This results in over 200 tons of dyes being discharged annually from the textile industry as wastewater that could cause severe environmental pollution[6]. The presence of dye in water, even at low concentrations, can cause health problems such as allergies, dermatitis, skin irritation, and cancer[7,8]. A concentration of dye higher than 1 mg/L makes water unsuitable for drinking due to potential harmful impacts on the reproductive system and liver functions[9]. In textile industries, various kinds of dyes have been used for many years including the basic, acidic, and neutral groups. Basic blue

[1]College of Engineering, Department of Environmental Engineering, Addis Ababa Science and Technology University, Addis Ababa, Ethiopia. [2]Department of Chemical and Metallurgical Engineering, University of the Witwatersrand, 1 Jorissen St, Johannesburg 2000, South Africa. [3]Institute for Nanotechnology and Water Sustainability (iNanoWS), College of Science, Engineering, and Technology, University of South Africa, Florida Science Campus, Johannesburg 1710, South Africa. ✉email: nuramsh@gmail.com

41 (BB41) dye also known as Benzothiazolium, is a cationic dye, whereas the Mordant Black 11 of Eriochrome Black T (EBT) is an anionic azo dye. These dyes have been used in the textile and tannery industries for the dyeing of various fabrics such as polyester, cotton, viscose, wool, nylon, and silk[10,11]. These dyes are classified as environmentally hazardous due to their potential to cause skin and eye irritation, mucosal tissue irritation, respiratory organ irritation, and liver damage upon prolonged exposure[10,11]. Despite their hazardous nature, these dyes are still widely used in the textile industry, particularly in developing countries. In many cases, the effluent containing these dyes is discharged directly into water streams without proper treatment[12]. This practice poses a significant risk to the environment and public health. Therefore, it is crucial to find effective methods for removing BB41 and EBT dyes from these effluents. Proper treatment of effluents containing these dyes is of utmost importance to prevent further contamination of water sources and minimize potential harm to both humans and the ecosystem. Developing efficient and sustainable methods for the removal of these dyes from wastewater is essential for maintaining a clean and safe environment.

Nowadays, various removal techniques have been used to remove dyes from various dyeing effluents. Among these, biological treatment[13], coagulation, flocculation, adsorption, chemical oxidation[14], and membrane separation[15,16], have proven to be effective. However, these commonly implemented methods are chemically intensive, complex, require skilled labor, and have high initial and maintenance costs and fouling issues[17,18]. Among all these techniques, adsorption is practically more feasible due to its greater accessibility, economical, ease of operation, and effectiveness to the maximum extent[19]. Activated carbons are widely used as adsorbents due to their large surface area, chemical properties, and versatility. However, their high production cost is a major obstacle to use at the industrial scale[20]. This is mainly due to the expensive materials and energy required in the production process[10,20]. To address this issue, researchers have introduced low-cost sources of activated carbon, such as agricultural waste and biomass materials. However, the production process, especially chemical activation methods, uses enormous amounts of corrosive chemicals and salts such as KOH, NaOH, $H_2SO_4$, and $H_3PO_4$, which can potentially enhance environmental pollution[2]. In recent times, biochar (BC) has emerged as a practical alternative to traditional adsorbents within the field of wastewater treatment. This shift is primarily attributed to its cost-effectiveness, widespread availability, and simple preparation process. Moreover, BC has proven to be highly effective in eliminating various pollutants from wastewater, making it a promising solution for pollution mitigation[19]. BC is a carbon-based adsorbent that is formed through the pyrolysis of biomass under limited oxygen or inert atmosphere. Various types of plant-based biomass and waste materials have been used including food waste, agricultural residues, and woody materials[21]. The utilization of BC as an adsorbent has become more prevalent due to its accessibility and affordability. It has high surface functional groups and a substantial specific surface area, making it an effective remover of pollutants[22]. The physiochemical properties of BC vary depending on the feedstock source and preparation conditions. Different feedstocks have different elemental compositions and thus exhibit different properties[23].

The plant Arundo donax is commonly known as giant reed which is a perennial grass that originally comes from Eastern Asia but has spread extensively around the world due to its invasive behavior. The plant has a rapid growth rate and is listed as one of the top 100 most harmful invasive alien species globally[24]. Giant reed is abandoned biomass and can be the low-cost raw material for BC preparation. Many studies have shown its great potential as a renewable precursor with a unique chemical composition for the preparation of high-grade adsorbent. BC produced from giant reeds was found to possess a significant surface area of 506.3 $m^2/g$ and a pore volume of 0.45 $cm^3/g$, demonstrating promising capabilities for water purification through adsorption mechanisms[26]. Previous studies have shown that BC derived from giant reed stems efficiently eliminates contaminants like heavy metals (Pb(II)[27], microcystin-LR[28], and ammonium ions[29], indicating its potential for wastewater remediation. On the other hand, the study of adsorption for the simultaneous removal of two pollutants from water and wastewater using BC developed from Giant reed was insignificant. The influence of the multipollutant on removal efficiencies and the interaction between the two contaminants under the same study condition was not thoroughly studied in the literature. Moreover, many of the studies conducted so far are mainly focused on either aqueous solution or simulated water/wastewater. However, this study intended to compare the findings under aquatic environments and real wastewater applications. Finally, to the best of the authors' knowledge, no studies have been reported on BB41 and EBT dye removals. Thus, this study was designed to synthesize giant reed BC and apply for the removal of those azo dyes from wastewater. Additionally, adsorption isotherms, adsorption kinetics, and reusability of the adsorbent material were thoroughly studied.

## Materials and methods

### Materials and reagents

A Giant reed was collected from the Addis Ababa Science and Technology University (AASTU) compound. This wild plant was collected by the researcher (Mohammednur Abdu) plant identification was performed by an expert and crossed check was done against the herbarium which is located at Addis Ababa University. This identification approach complies with relevant institutional, national, and international guidelines and legislation. Basic blue 41 and EBT were used as model dye pollutants. The chemicals used in this study were of analytical grade. The primary chemicals used in this study were hydrochloric acid, sodium hydroxide, and sodium chloride.

### Textile effluent collection and characterization

The textile wastewater effluent employed in this study was obtained from the KK textile industry located in Ethiopia A portion of the textile wastewater was gathered utilizing a grab sample technique, and then the collected effluent was subsequently preserved at a temperature of 4 °C to prevent any undesired alterations. The wastewater effluent was then subjected to characterization through the process using known methods The analyzed

parameters consisted of pH, temperature, electric conductivity (EC), turbidity, total dissolved solids (TDS), biochemical oxygen demand ($BOD_5$), chemical oxygen demand (COD) and color as shown in the Table1.

## BC preparation

With regards to information on the voucher specimen and its identification has been included in this manuscript. Specifically, permission to collect Giant reed (Arundo donax) in Ethiopia was obtained from the National Herbarium of Addis Ababa University (ETH), supported by a letter from Addis Ababa Science and Technology University. The plant material was formally identified by Dr. Weldemariam Seifu, a botanist at Addis Ababa University. The voucher specimens with no voucher (ID) were then stored in Addis Ababa University's National Herbarium (ETH). The use of plant parts in this study complies with international, national, and institutional guidelines. The Giant reed (Arundo donax L.) was crushed and air-dried, then dried in an oven at 105 °C for 24 h. The dried biomass was then milled using a hammer mill and screened through an 80—120 mesh sieve. The Giant reed BC was prepared by slow pyrolysis with a heating rate of 10 °C /min at 600 °C for 2 h in a muffle furnace under a flow rate of 5 L/min nitrogen atmosphere. After cooling to room temperature, the obtained BC was ready for use.

## BC characterization

The adsorbent characterization is a key factor in wastewater treatment because it gives an insight into the material characteristics and determines if the proposed material will suit the target pollutant. Different techniques have been used to determine the characteristics of the BC such as proximate analysis which includes moisture content, volatile matter, ash content, and fixed carbon was performed according to BS EN ISO standard methods (18,123, 2015; 18,134–3, 2015; ISO, 2015). The BC's point of zero charge (pHpzc) was determined through the salt addition method using a 0.01 M NaCl solution spanning a pH range from 3 to 11 (Mahmood et al., 2011). The BET-specific surface area and pore structure of BC were determined using the NOVA 4000E BET analyzer. The surface of functional groups was analyzed using an infrared spectrometer (iS50 FTIR). Molecular interactions and chemical structure were examined through Raman analysis with a WITec Raman spectrometer. The analysis is carried out at a magnification of 100X using a 532 nm laser emitting power of 5 mW. The BC's crystal structure was analyzed using X-ray diffraction spectroscopy (SHIMADZU XRD-6000). The surface morphology was studied through Scanning Electron Microscopy (SEM) (JSM-IT300 Joel, Tokyo, Japan). The SEM coupled with an energy-dispersive X-ray (EDX) detector (Oxford X-MAXN) was employed to confirm the presence of BC elements. the thermal stability of BC is assessed using a thermogravimetric analyzer (TGA 55-TA).

## Adsorption experiments

The batch adsorption experiments were carried out in triplicate to investigate the efficiency of BC adsorbent for the removal of BB41 and EBT dyes accordingly. At the outset, a stock solution of 1 L containing 100 mg/L of EBT and BB41 dye was prepared. The prepared stock solution was used throughout the study to prepare different concentrations. The adsorption process is affected by various parameters, including initial concentration, adsorbent dosage, solution pH, and contact time[30]. To achieve optimal adsorption performances, it is crucial to carefully optimize these parameters. The process of optimization in adsorption studies involves varying one parameter at a time while keeping all other parameters constant In this study, the effect of the pH of the solution (ranging from 3 to 11), BC dosage (ranging from 2 to 5 g/L in a 100 mL solution), initial dye concentration (ranging from 10 to 50 mg/L), and contact time effect, ranged from 20 to 100 min for BB41 and EBT dye, was examined. The solutions were filtered and dye concentrations were measured at 617 nm and 534 nm using a Biochrom Libra S80 PC UV/ VIS spectrometer Eq. (1) was employed to determine the adsorbate removal percentage (%)[31].

| No | Parameter | Observed values |
|---|---|---|
| 1 | Temperature | 45 °C |
| 2 | pH | 5.61 |
| 3 | Color | 106 Pt–Co |
| 4 | EC | 1605 µS/cm |
| 5 | Turbidity | 48.55 |
| 6 | TDS | 1105 mg/L |
| 7 | $BOD_5$ | 350 mg/L |
| 8 | COD | 928 mg/L |
| 9 | BB41 Dye conc | 5.7 ± 0.3 mg/L |
| 10 | $NO_3^-$ | 11.9 mg/L |
| 11 | $SO_4^{2-}$ | 47 mg/L |
| 12 | $NH_4^+$ | 15 mg/L |
| 13 | $PO_4^{3-}$ | 3.5 mg/L |

**Table 1.** Physiochemical characteristics of the textile wastewater.

$$\%\mathrm{Re}moval = \left(\frac{C_o - C_e}{C_o}\right) \times 100 \tag{1}$$

Where $C_o$ and $C_e$ represent the initial and final dye concentrations (mg/L).

## Adsorption isotherms

The adsorption isotherms study was conducted using 250 mL conical flasks filled with 100 mL of dye solution. Initial concentrations ranged from 10 to 50 mg/L for BB41 and EBT dyes. The pH levels were set at 3 for EBT dye and 9 for BB41 dye. A BC dose of 4 g/L was added and left for 60 min. The solutions were then filtered, and the dye concentrations were measured at 617 nm and 534 nm using a UV–vis spectrophotometer. Following this, the collected data underwent analysis using Langmuir, Freundlich, Temkin, and Dubinin-Radushkevich adsorption isotherm models, widely used in water and wastewater analysis.

Langmuir and Freundlich isotherm model equations:

$$\frac{1}{q_e} = \frac{1}{q_{\max}} + \frac{1}{K_L q_{\max} Ce} \tag{2}$$

$$RL = \frac{1}{1 + K_L Ce} \tag{3}$$

$$\ln qe = \ln k_f + \frac{1}{n} \ln Ce \tag{4}$$

where qe represents adsorbed dye at equilibrium; $q_m$ is the maximum adsorption capacity; and $K_L$ denotes the Langmuir constant in l/mg. The Langmuir adsorption isotherm model explains the monolayer surface of adsorption sites and the lack of interactions among adsorbate molecules. Equation (3) shows the dimensionless separation factor constant ($R_L$) for estimating Langmuir's isothermal feasibility[20]. Freundlich's model uses $K_f$ for adsorption capacity and 1/n for adsorption intensity.

Temkin isotherm model equation:

$$qe = \frac{RT}{bT} \ln KT + \frac{RT}{bT} \ln Ce \tag{5}$$

where bT is the Temkin constant in kJ/mol, K is the equilibrium binding constant in l/g, T is the temperature in Kelvin (K), and R is the gas constant $8.314 \times 10^{-3}$ kJ/(mol K).

Dubinin-Radushkevich (D-R) isotherm model equation:

$$\ln qe = \ln qm - \beta\varepsilon^2 \tag{6}$$

$$\varepsilon = RT \ln\left(1 + \left(\frac{1}{Ce}\right)\right) \tag{7}$$

$$E = \frac{1}{\sqrt{2\beta}} \tag{8}$$

where b represents a constant to the free energy of adsorption (expressed $mol^2/J^2$). the parameter qm denotes saturation adsorption capacity (in mg/g), Ɛ stands for the Polanyi potential, R (J/mol K) is the gas constant, T denotes temperature in kelvin, and E free energy of adsorption (in kJ/mol). The E values provide important information about the adsorption mechanism like chemical ion exchange or physical adsorption.

## Adsorption kinetics

The adsorption kinetics experiment was conducted by considering optimum parameters. Initial dye concentrations of 30 mg/L, a BC dose of 4 g/L, pH values of 3 for EBT dye and 9 for BB41 dye, and a 60-min contact period were set, respectively. Approximately 5 mL of each dye solution was taken at intervals of 10 min until the end of the 60-min period. The concentrations of BB41 and EBT were assessed at wavelengths of 617 nm and 534 nm, using a UV–vis spectrophotometer. Subsequently, the obtained data underwent scrutiny using pseudo-first and pseudo-second-order kinetic models, denoted by Eqs. (9) and (10).

$$\ln(\mathrm{qe} - \mathrm{qt}) = \ln(\mathrm{qe}) - \mathrm{k}_1 t\# \tag{9}$$

$$\frac{1}{\mathrm{qt}} = \frac{1}{\mathrm{k}_2 \mathrm{q}^2 \mathrm{e}} + \frac{1}{\mathrm{qe}} t\# \tag{10}$$

where qe (mg/g) and qt (mg/g) adsorbed dye at equilibrium at time t; $k_1$ is the rate constant for the pseudo-first-order model and $K_2$ is the rate for the pseudo-second-order adsorption (g/mg.min).

### Adsorbent regeneration

Regeneration of the adsorbent is essential for practical applications. Once adsorption equilibrium is attained, the adsorbent needs to be recycled by desorbing the adsorbed molecule. The experiments were conducted using 4 g/L of dye-loaded BC in 100 mL of 0.1 M HCl and shaking at 180 rpm for 2 h. After being cleansed with deionized water, the BC was dried in the oven at 80 °C for 1 h and reused again. The process was carried out in seven cycles to examine the BC's adsorption efficacy[32].

## Result and discussion

### BC characterization

*Proximate analysis*

The results of the proximate analysis of giant reed BC are given in Table 2. These results are composed of the moisture content of 3.94%, fixed carbon of 80.37%, volatile matter of 11.85%, and ash content of 3.84%. Fixed carbon and ash content are the most important proximate analytical metrics for assessing the quality of adsorbent materials. A high proportion of fixed carbon and low ash content are regarded as advantageous attributes of quality BC due to their role in enhancing its efficacy as an adsorbent material.[20]. The fixed carbon content is the amount of carbon left in the BC after the volatile components have been removed during pyrolysis. A high fixed carbon content indicates that the BC has a greater capacity to adsorb different types of pollutants, which is important for mitigating water-soluble pollutants from wastewater[33]. On the other hand, ash content refers to the inorganic minerals that are left behind in the BC after pyrolysis. Ash content can highly affect the quality of BC. A low ash content is desirable because excessive ash can interfere with the BC's adsorption efficiency. High levels of ash content can result in clogging of pores within BC, leading to a decrease in surface area. Consequently, this can reduce the adsorption capacity of the BC[34]. However, the value of the proximate analysis is not only determined by the precursor nature but also greatly influenced by carbonization processes[34]. It is important to consider both the precursor nature and carbonization processes when evaluating the proximate analysis value of a material, as they both play crucial roles in determining the overall quality and characteristics of the carbon product. Table 2 shows the properties proximate value of BC from giant reeds are impacted by the temperature of pyrolysis. The fixed carbon content rises with higher pyrolysis temperatures, while the ash content decreases. However, it was found that the ash content is notably high in BC produced at 500 °C and 800 °C compared to the BC studied in this research[26]. It is important to note that the results may vary depending on the nature and growing conditions of the giant reed plant. Based on the obtained results the Giant Reed BC is a good quality adsorbent material and can be utilized for a variety of pollutant treatments.

*Point of zero charge ($pH_{pzc}$)*

The pHpzc is an important parameter in understanding the surface chemistry of adsorbent material, as it can affect the adsorption behavior of contaminants in water. Understanding the pHpzc of BC and other adsorbent materials is essential for developing efficient and effective water remediation techniques to remove particular contaminants. By considering the surface charge properties of the adsorbent material with the pH of the solution, the adsorption process can optimize for maximum contaminant removal. At pH values below the pHpzc, BC attracts negatively charged contaminants, while above the pHpzc, it attracts positively charged contaminants[36]. As shown in Fig. 1, the pHpzc of the BC is approximately 8.62, indicating that the surface charge of the BC is positive in a solution with a pH lower than 8.62, and negative in a solution with a pH higher than 8.62. BC exhibited a slightly higher pH level at the pHpzc values, which could be attributed to the release of alkaline salts from the feedstock during the high-temperature pyrolysis process[37]. Additionally, it has been reported by researchers that most BCs produced through slow pyrolysis were alkaline[38,39].

*XRD analysis*

XRD is a technique that allows to analysis of the degree of crystallinity of the BC. The XRD result of the study is presented in Fig. 2. According to the diffractogram result, two wide peaks were detected at 2θ that ranged from 20° to 30° and 40° to 50°, which indicates the presence of amorphous and crystalline graphene diffraction. The broad peak observed at an angle of 23.5 ° represents the crystal plane index C (002), indicating the alignment of aromatic and carbonized structures. Similarly, the significant peak at 43.5 ° corresponding to C (100) indicates the diffraction patterns of graphitic and hexagonal carbons[40]. The presence of all the peaks in the XRD pattern of the BC indicated the successful formation of the desired porous graphitic carbon. The development of a porous structure of graphitic carbon in BC holds significant value due to its diverse range of practical applications. The porous nature of the material allows for increased surface area, which is beneficial for the adsorption of different types of pollutants[41]. Additionally, the graphitic carbon structure provides mechanical and thermal stability,

| Biomass type | Ash content | Fixed carbon | Volatile content | Moisture content | |
|---|---|---|---|---|---|
| Giant reed (500 °C) | 6.85% | 75.20% | 14.72% | 3.23% | [35] |
| Giant reed (800 °C) | 6.20% | 81.30% | 7.48% | 5.02% | [35] |
| Coconut flesh waste | 8.19% | 79.09% | 12.71% | 2.36% | [33] |
| Giant reed (600 °C) | 3.84% | 80.37% | 11.85% | 3.94% | This study |

**Table 2.** Proximate analysis BC of giant reeds.

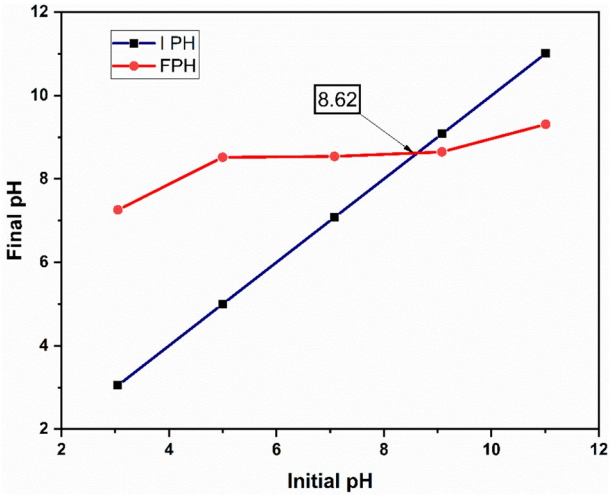


**Figure 1.** Point of zero charges ($pH_{pzc}$) of BC.

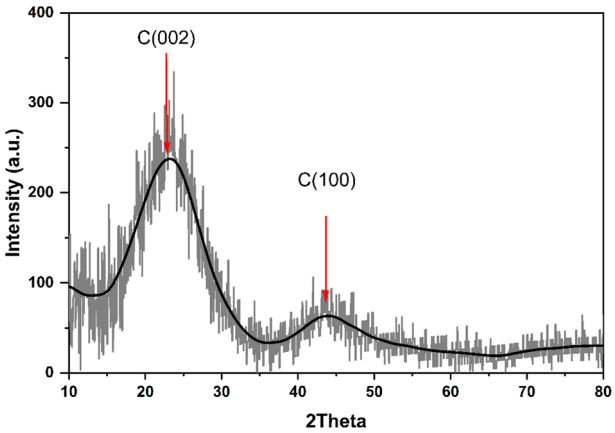


**Figure 2.** XRD analysis of BC.

making it suitable for adsorption applications[42]. Similar X-ray diffraction (XRD) results were reported in the literature for BC produced from peanut shells and sugarcane bagasse[43], rice husk[44], Douglas fir[45], and miscanthus[40].

*FTIR analysis*

The FTIR spectra of giant reeds biomass and BC are shown in Fig. 3. The broad peak centered at 3300 $cm^{-1}$ described the O–H stretching of the hydroxyl groups in cellulose, hemicellulose, and the hydration water component of biomass. The medium broad peak observed at 3000–2800 $cm^{-1}$ indicates C–H stretching of hemicellulose and cellulose. The medium peaks from 1760–1690 and 1320–1210 $cm^{-1}$ ascribed C = O stretching of carbonyl and carboxyl groups. From 1690–1610 $cm^{-1}$ C = C stretching of alkene and aromatic groups. 1465–1380 $cm^{-1}$ indicates C-H bending of alkane. The prominent band centered at around 1000 $cm^{-1}$ in the spectra of the biomass assigned to C–O and C–C stretching or C–OH also indicates the sign of cellulose, hemicellulose, and lignin part of the biomass[46]. The decomposition of cellulose and hemicellulose is also confirmed by the disappearance of the prominent band at 3300 $cm^{-1}$, 3000–2800 $cm^{-1}$, and 1000 $cm^{-1}$ in the spectra of the biomass, the pyrolysis temperature determines the thermal decomposition of these groups. The changes in the infrared spectra are linked to the gradual elimination of oxygen-containing substances such as cellulose and hemicellulose[46]. The spectra of BC clearly show the bands associated with the aromatic C = C stretching (1640 $cm^{-1}$) and C = C bending (840–790 $cm^{-1}$) aromatic structure of the BC this could provide additional evidence of the graphitization process to XRD results. According to the graph, the disappearance of BC peaks could indicate the elimination of functional groups from the surface of BC. This may result in decreased adsorption efficiency. However, eliminating oxygen-containing functional groups can increase the porosity of BC. The porous nature of BC allows for an increase in surface area, directly influencing an adsorbent's adsorption capacity. Adsorbents with larger surface areas tend to have greater adsorption capabilities, as pollutants can be more efficiently adsorbed on higher surfaces, due to having more accessible adsorption sites[18].

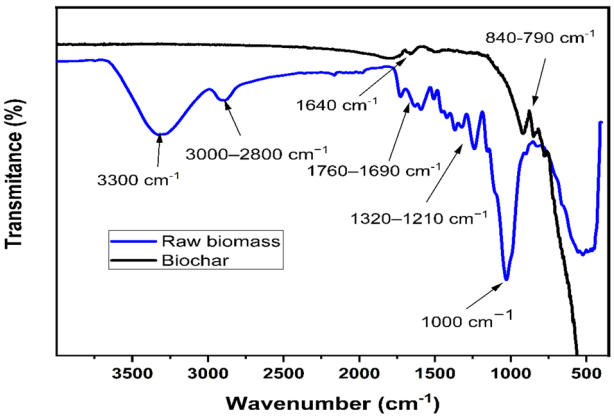


**Figure 3.** FTIR spectrum for Giant reed biomass and BC.

*Raman spectroscopy analysis*

The BC chemical and crystal structures were examined using non-destructive Raman spectroscopy. The Raman spectra of BC are displayed in Fig. 4. There are two prominent peaks corresponding to the D band (around 1353 $cm^{-1}$) and the G band (at 1590 $cm^{-1}$). The D band corresponds to the in-plane vibration of $sp^2$-carbon structures with structural defects and $sp^2$-bonded graphitic structures of double bonds of giant reed BC and the G band is due to in-plane C–C deformation[40,47]. However, The G band has been attributed to BC aromatic ring systems[48]. The BC material typically shows a discernible 2D band at around 2826 $cm^{-1}$ which corresponds to the overtone of the D band[49]. The 2D band is useful in identifying monolayer graphene from multilayer graphene because it is very perceptive to stacking. Monolayer graphene has a peak at 2679 $cm^{-1}$, whereas multilayer graphene has a larger peak at a higher wavenumber[40]. In this study, the 2D peak of giant reed BC is observed at 2826 $cm^{-1}$ which confirmation of a multi-layered graphitic carbon structure. BC with a higher wavenumber and wider 2D peak indicates a multi-layered graphitic carbon structure. This is additionally supported by the XRD results provided in this study.

*BET analysis*

The specific surface area and volume of BC were analyzed using the surface area analyzer. The result indicated that the BET surface area and volume are 428.98 $m^2/g$ and 0.0854 $cm^3/g$, respectively. This indicates that the giant reed can be an effective adsorbent since it has a higher surface area and is also abundant and environmentally benign. Adsorbates can be adsorbed more efficiently on higher surfaces as they have more accessible adsorption sites. The adsorption capacity of an adsorbent is directly affected by its surface area. Adsorbents with larger surface areas tend to have greater adsorption capabilities. In comparison to many locally prepared BC, giant reed BC has a higher specific surface area than recently reported BC like C. glomerata-BC (6.45 $m^2/g$), G. gracilis-BC (2.11 $m^2/g$)[32], rice husk (364.2 $m^2/g$) and coconut coir (329.7 $m^2/g$)[44]. BC produced from similar precursor materials was found to exhibit BET surface areas of 345.92 $m^2/g$ and 506.27 $m^2/g$ when subjected to pyrolysis at 500 and 800 °C[35]. The BC's surface area after pyrolysis at 800 °C (506.27 $m^2/g$) was observed to be greater than the prepared BC's surface area (428.98 $m^2/g$), as documented in the same study. This implies that as the temperature rises, the surface area of the BC will increase.

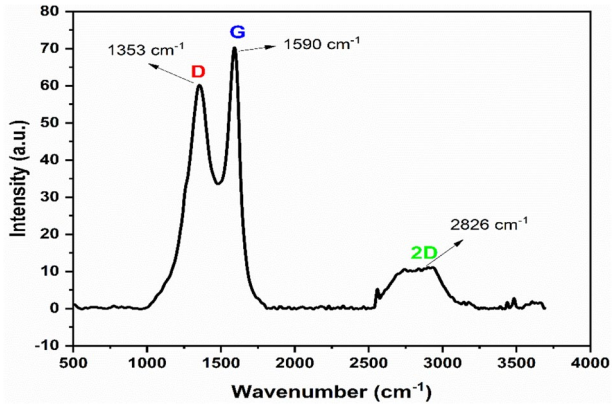


**Figure 4.** Raman spectrum for BC.

*SEM- EDX analysis*

The utilization of SEM is crucial in the analysis of an adsorbent's morphological structure and physical properties. As depicted in Fig. 5, the BC exhibits a surface that is highly porous, heterogeneous, and coarse, displaying a rough microstructure. The SEM image provides clear evidence of morphological fractures on the surface of the adsorbent. This porous structure is likely formed as a result of the volatilization of cellulose, hemicellulose, and lignin materials during the pyrolysis process of the biomass[50]. The presence of a highly porous structure creates a favorable environment for the adsorption of various types of pollutants. Considering the porous nature of the giant reed BC, it offers a significant surface area to volume ratio, making it an effective adsorbent for the removal of dye pollutants from wastewater. Additionally, an EDX analysis was conducted to identify the elements present in the BC adsorbent and their distribution. Figure 5b illustrates the elements found in the adsorbent, with their respective KeV values displayed on the x-axis. It was observed that the BC constituents are carbon (90.1%), oxygen (8.1%), potassium (1%) calcium (0.6%), and magnesium (0.3%). The high distribution of carbon can be attributed to the BC's plant-based origin of the thermal decomposition of cellulose and hemicellulose constituents in the giant reed plant, resulting in the formation of a solid by-product (BC) with a more carbonaceous and porous structure.

*TGA analysis*

TGA studies were performed to determine the BC thermal stability. A good absorbent is one with high thermal stability under the influence of temperature and time[51]. TGA analysis of the BC was conducted in the temperature range of 30 to 900℃ under a nitrogen atmosphere at a heating rate of 20°C/min. As shown from Fig. 6 about 3.1% of the weight loss of BC occurred between 50–100℃ possibly due to the evaporation of physically adsorbed water. This shows that the surface of the BC material holds a small amount of water. Between 100–500 °C the mass of the BC remained constant; this may indicate that the cellulose and hemicellulose part of the BC was significantly eliminated during the pyrolysis process. This also indicates the BC was thermally stable and indicates the BC has good adsorbent properties[51]. As the temperature increases from 500–850 °C, the mass of the BC significantly decreases. About 55% of the BC fraction evaporates between 500 and 850 °C, which indicates

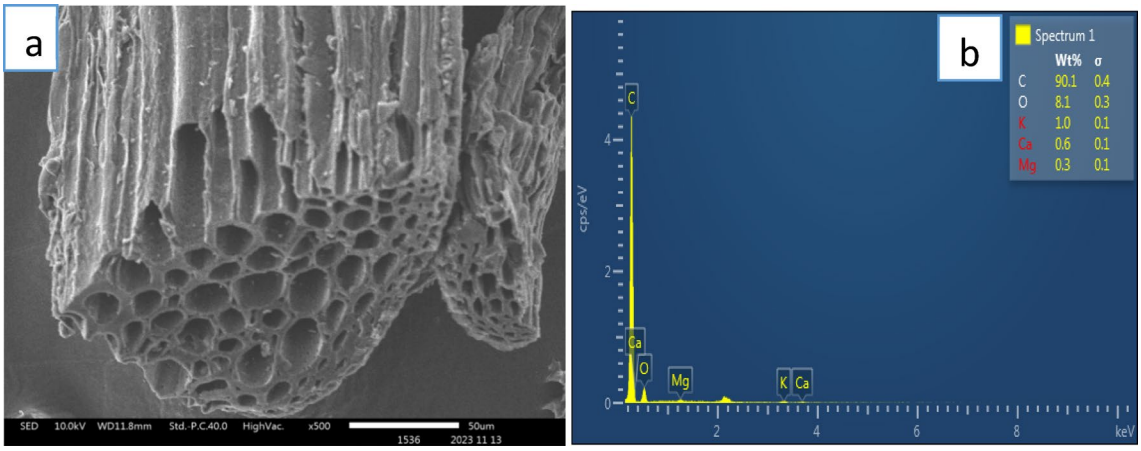


**Figure 5.** (**a**) SEM images and (**b**) EDX analysis of BC adsorbent.

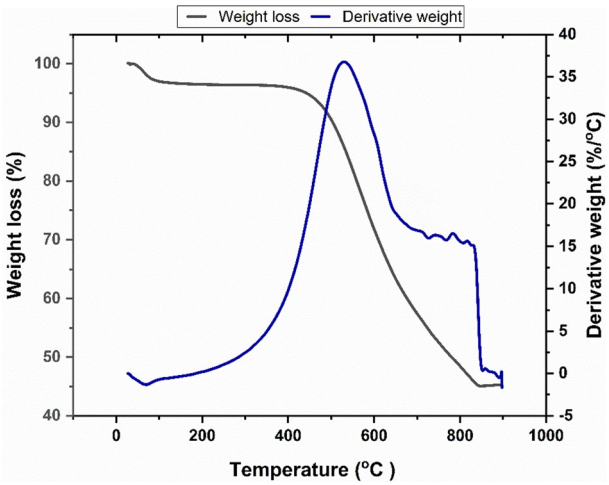


**Figure 6.** The TGA analysis of BC.

that a fraction of organic components like cellulose and lignin can be decomposed. However, at a temperature of about 8500–900 °C, the mass of the BC remained constant which indicated 45% of the BC's composition remained stable from 850–900 °C, This indicates that the presence of graphitic carbon fraction which is similar to TGA analysis of crab shell BC[52].

## Adsorption study

### Effect of solution pH

The pH plays a significant role in the adsorption process and requires careful investigation. The investigation of pH is crucial in the adsorption process as it impacts various aspects such as the structure, surface charges, dissolution, and ionization of the adsorbent. pH plays a significant role in determining the efficiency and effectiveness of adsorption processes[53]. In this study we utilized the giant reed BC adsorbent for the adsorption of BB41 and EBT dyes from aqueous solution, the pH was investigated within the range of 3 to 11. Throughout the pH investigation, all other parameters such as initial concentration, BC dose, and contact time were kept constant at 20 mg/L, 2 g/L, and 60 min respectively. As shown in Fig. 7 the adsorption of BB41 (cation) was favorable in a basic medium whereas the adsorption of EBT (anion) dye was favorable in an acidic media solution. This phenomenon can be attributed to the fact that at higher pH levels, the surface charge of the BC becomes more negative, which attracts positively charged molecules like BB41 dye. This increased electrostatic interaction between the BC and BB41 results in a higher adsorption capacity for the cationic dye. On the other hand, the adsorption of the anionic dye EBT decreases at higher pH levels due to repulsion between the negatively charged BC surface and the negatively charged dye molecules. This shows the significance of the electrostatic interactions between the adsorbent and the dye molecules. Furthermore, the PZC principle plays a vital role in determining the adsorption behavior of dyes on BC surfaces, highlighting the significance of pH in controlling the efficiency of dye removal in wastewater treatment processes[30]. Therefore, this could be the primary mechanism of adsorption. The results indicated that the highest BC adsorption efficiency was 86.5% at pH 9 for BB41 dye and 65.4% at pH 3 for EBT dye. This result is also supported by[54] for BB41 and EBT[55].

*Effect of adsorbent dose*

The study of the adsorbent dosage is essential to avoid excess adsorbent usage after reaching the equilibrium phase. According to the adsorbent dosage analysis result from Fig. 8, the percentage of adsorption of both anionic(EBT) and cationic(BB41) dyes increased when the adsorbent dose increased. The removal percentage of BB41 increased from 79.5% to 98.6% as the BC dosage was increased from 2 to 4 g/L. Similarly, the removal percentage of EBT also showed an increase, rising from 65.4% to 82.7% with the same increase in BC dosage. The efficiency of adsorption increases as more adsorbent is used. This suggests that there are more active sites or surface areas available for the interaction between the BC and the dye molecules. Having more active surface sites increases the percentage of dye removal[18]. However, the adsorption efficiency did not significantly increase above 4 g/L adsorbent dose (98.6%) and (82. 5%) for both dye BB41 and EBT dyes. This may be due to the formation of aggregates and overlapping of the adsorbent particles in the solution. The aggregation and overlapping of adsorbent particles can result in a reduction of the available surface area for adsorption. This, in turn, can hinder the diffusion of dye molecules towards the adsorbent surface[56]. When the adsorbent dose is increased beyond a certain limit, it can further contribute to the decrease in adsorption efficacy due to diffusion limitation[20].

*Effect of initial dye concentration*

Figure 9 displays the removal efficiency of BB41 and EBT dyes at different initial dye concentrations. The results show that the removal efficiency of BB41 remained stable between 10 mg/L and 30 mg/l, but declined from

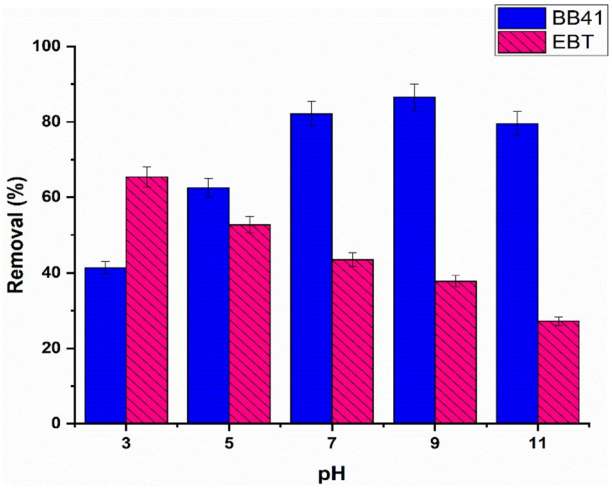


**Figure 7.** Effect of pH, 2 g/L of adsorbent, and a contact time of 60 min on the dyes BB41 and EBT at a concentration of 20 mg/L.

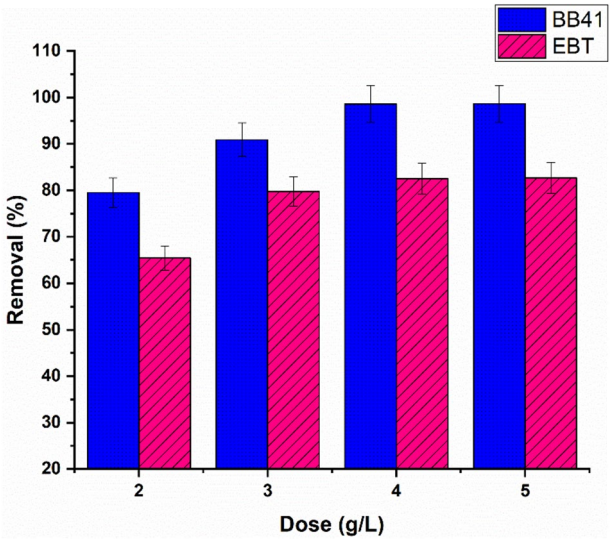


**Figure 8.** Effect of adsorbent dose at pH levels of 9 and 3 for BB41 and EBT dyes, with a dye concentration of 20 mg/L and a contact time of 60 min.

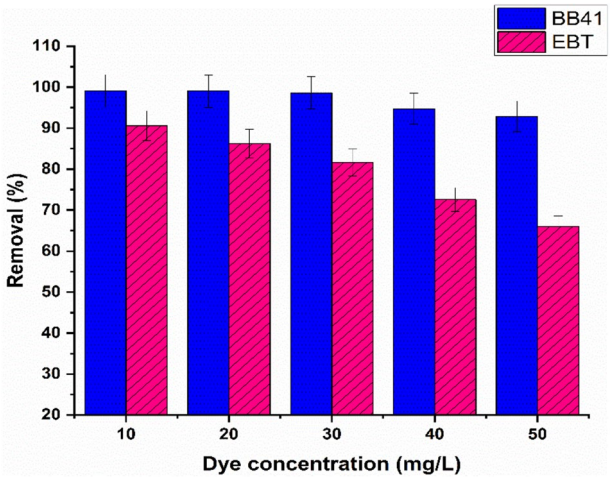


**Figure 9.** Effect of the initial dye concentration at 4 g/L adsorbent dose, under pH conditions of 9 and 3 for BB41 and EBT dyes, and a contact time of 60 min.

98.6% to 92.9% as the concentration rose from 30 mg/L to 50 mg/L. Conversely, the removal efficiency of EBT decreased from 90.6% to 66.0% as the dye concentration increased from 10 mg/L to 50 mg/L. The reduction in percentage removal was observed as the initial concentration of dye increased. This can be attributed to the increase in the number of dye molecules, resulting from the higher initial concentration, which in turn limits the availability of adsorbent sites[18]. Additionally, the rate at which dye molecules pass from the bulk solution to the surface of the adsorbent is reduced as the initial concentration increases.[57,58]. In another study, it was found that the removal percentage of methylene blue decreased from 10 to 50 mg/L at the initial concentration. The highest percentage of removal, 98%, was achieved at a lower initial concentration of 10 mg/L, whereas the lowest percentage of removal was recorded at 50 mg/L[58]. BC exhibited the highest adsorption capacity for BB41 and EBT dyes at concentrations of 30 mg/L and 20 mg/L, respectively. Furthermore, the results suggest that the BC adsorbent possesses specific active sites for the adsorption of BB41 and EBT dyes. This BC could be a promising solution for removing these specific dyes from wastewater, as it has a high affinity for them even at relatively low concentrations. The presence of specific active sites on the BC surface indicates that it has been specifically designed or naturally evolved to target these particular dyes, making it a highly effective and efficient adsorbent for their removal. This could have significant implications for water treatment processes, as BC could potentially be used to effectively remove these harmful dyes from contaminated water sources, improving water quality and environmental sustainability.

*Effect of contact time*

Figure 10 illustrates the elimination rate of BB41 and EBT dyes at different contact durations under specific circumstances. These circumstances involve a dye concentration of 30 mg/L, pH levels of 3 and 9 for the EBT and BB41 dyes, and a BC dosage of 4 g/L. The results demonstrated that the adsorption process exhibited a rapid rate within the first 20 min, leading to the adsorption of approximately 96.0% of BB41 and 62% of EBT dye during this period. This can be attributed to the availability of vacant surface sites on the adsorbent, which facilitated the interaction between the dye molecules and the active sites on the BC[59]. After 40 min, the removal efficiency increased to 97.3% for BB41 and 71.5% for EBT dye. Furthermore, at the 60-min mark, a significant removal of 98.0% for BB41 and 80.30% for EBT dye was achieved. After 60 min, the adsorption capability remained relatively stable, suggesting that the dye had achieved equilibrium on the BC. However, beyond this point, the removal efficiency did not significantly increase, Maybe this is because all the available active sites are saturated[18].

*Adsorption isotherms*

The experimental data was examined using different isotherm models, including Dubinin-Radushkevich (D-R), Temkin, Langmuir, and Freundlich as indicated in Fig. 11. Table 3 summarizes the values obtained from these model equations. Table 3 displays the highest $R^2$ values for the Langmuir isotherm model, with $R^2$ values of 0.995 and 0.992 for BB41 and EBT dyes, respectively. These findings suggest that both dyes exhibit a strong fit with the Langmuir isotherm model. The Langmuir model proposes that dye adsorption occurs in a monolayer, with no interactions between the adsorbed molecules and the adsorption energy uniformly dispersed across the adsorbent surface. The model shows, the BC maximum adsorption capacity of 58.48 mg/g for BB41 dye and 9.09 mg/g for EBT dye. This indicates that the BC has a strong affinity for both cationic and anionic dyes. It is important to note that BB41 dye has a higher affinity for adsorption compared to EBT dye. The adsorption favourability of BB41 and EBT dyes on BC was also assessed based on the RL value. The RL value provides insights into the nature of adsorption. If $RL > 1$, it indicates an unfavorable process. $RL = 1$ indicates a linear relationship. When $0 < RL < 1$, it indicates favorable adsorption and $RL = 0$ indicates irreversible adsorption[60]. According to Table 2, the RL values for BB41 and EBT dyes are 0.15 and 0.087, respectively, falling within the range of $0 < RL < 1$. This suggests that the Langmuir isotherm was favorable for the adsorption of both cationic (BB41) and anionic (EBT) azo dyes. Recent research also reported anionic Congo red and EBT dye adsorption was compatible with the Langmuir isotherm model[61,62]. A similar study on BB41 dye also reported that adsorption was fitted with the Langmuir isotherm model[60]. The $q_{max}$ values of BB41 and EBT dyes are 58.48 mg/g and 9.09 mg/g respectively. The result Indicates that the BC adsorbent has good adsorption affinity for both cationic and anionic dyes, however, the BB41 dye has more adsorption affinity compared to the EBT dye. The BB41 dye has higher adsorption affinity compared to the EBT dye because of its single positive charge, which allows it to occupy only one negative charge on the BC surface. On the other hand, the EBT dye is triprotic, containing one sulfonic ion and two hydroxyl group negative charges, and can occupy multiple active sites with positive charges on the BC surface[63]. The adsorption capacity of BC may be influenced by the available charge of the molecule, potentially leading to a reduction in the adsorption capacity of the BC surface.

*Adsorption kinetics*

The Adsorption kinetics is the most essential parameter to evaluate the efficiency, potential application of the adsorbents, and feasibility of the adsorption system. Pseudo-first-order and pseudo-second-order kinetics models were applied to analyze the BB41 and EBT dye absorption kinetics on the BC shown in Fig. 12. Table 4 displays the adjusted correlation coefficient ($adjR^2$) values for the BB41 dye and EBT dye for the pseudo-first-order and pseudo-second-order kinetics models. The $adjR^2$ values for the BB41 dye are 0.909 and 0.999, and for the EBT dye, are 0.886 and 0.990. These results indicate that the pseudo-second-order model is more suitable for both

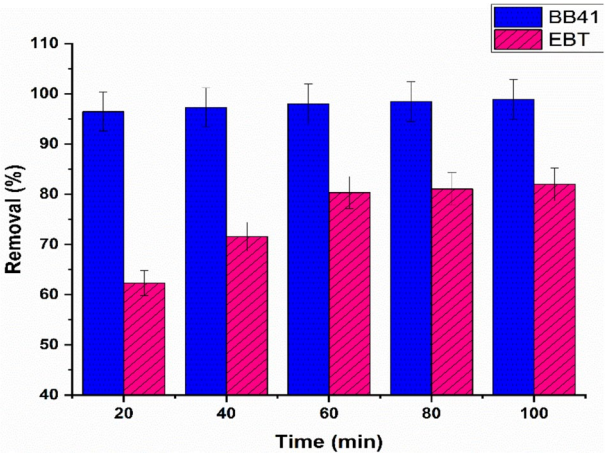


**Figure 10.** Effects of contact times at a 4 g/L dosage of adsorbent under pH levels of 9 and 3 for BB41 and EBT dyes, with a dye concentration of 30 mg/L.

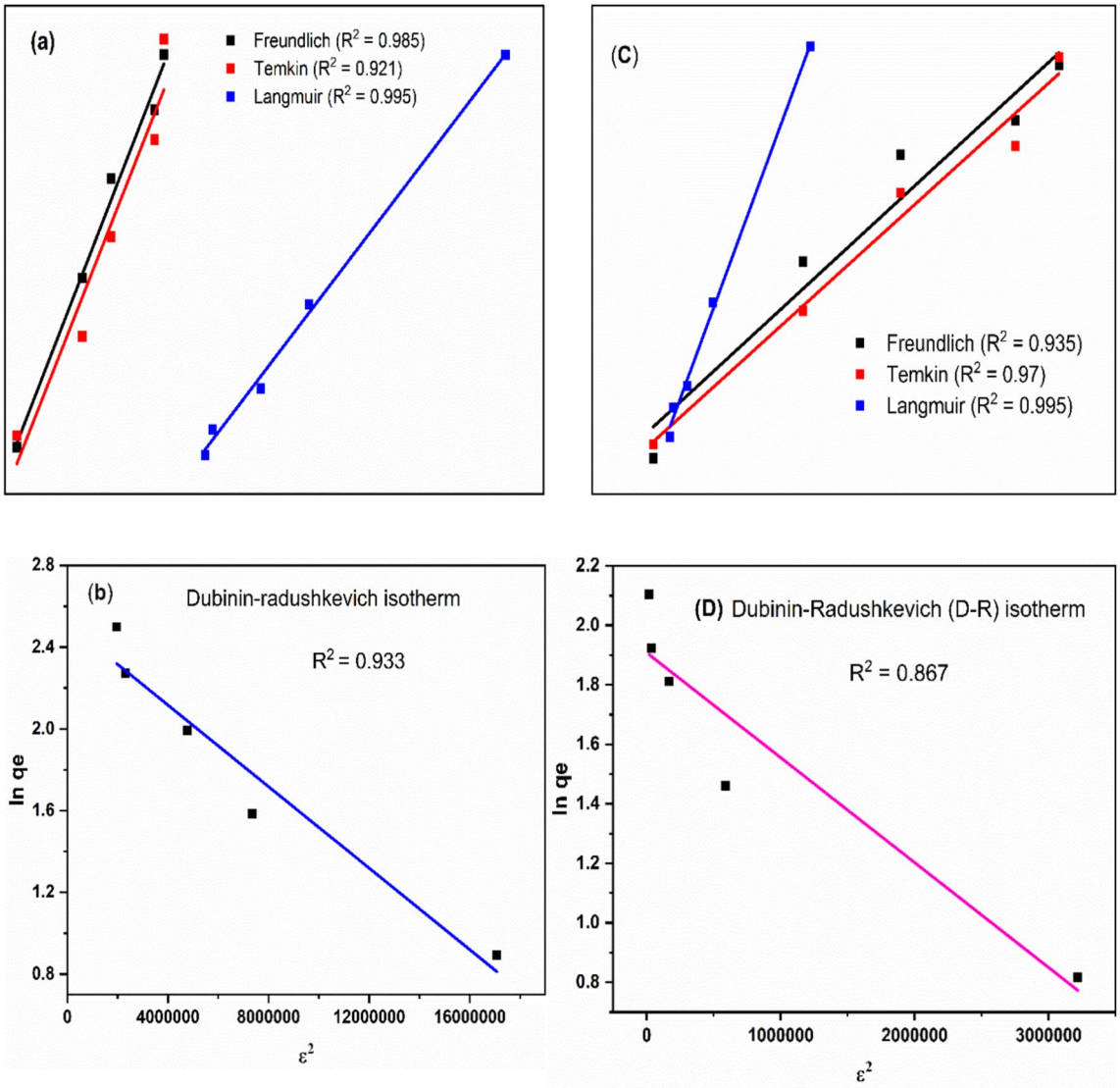


**Figure 11.** Adsorption isotherm model analysis graph (a and b) for BB41 and (c and d) for EBT dye.

cationic (BB41) and anionic (EBT) dye adsorption onto BC. This also suggested that the adsorption of BB41 and EBT dyes was involved in the chemical adsorption system.

*Regeneration and reusability study*

In this study, the regeneration BC was performed with 0.1 M HCl for five cycles. BC adsorbent was washed with 0.1 M HCl in each cycle, and the results are presented in Fig. 13. At first recycling process, the adsorption efficiency of BC was not reduced for both BB41 and EBT dyes; however, after the fourth regeneration process, the BC adsorption efficiency was slightly reduced for both BB41 (cationic) and EBT (anionic) dye. The result shows the adsorption efficiency decreased by 3.9% and 3.5% for BB41 and EBT dyes after four recycling processes respectively. However, After seven cycles, the removal efficiency of the BC decreased from 98.6% to 58.2% for BB41 and from 82.6% to 39.6% for EBT dye. The giant reed BC adsorbents demonstrate good adsorption and regeneration efficiency for both cationic and anionic dyes. This suggests that the Acid desorption method is favorable for both Cationic (BB41) and anionic (EBT) azo dyes. Due to raw material availability and the simplicity of the production process, giant reed BC can be considered as an alternative potential adsorbent for practical application.

*Application on real textile wastewater*

The adsorption experiment was carried out in duplicate to assess the effectiveness of BC in removing BB41 dye, color, turbidity, and COD from actual textile effluent. The initial concentrations of BB41 dye, color, turbidity, and COD in the textile effluent were 5.7 mg/L, 106 Pt–Co, 48.55 NTU, and 928 mg/L, respectively. After one hour of treatment with a BC dose of 4 g/L, around 5.14 mg/L of BB41 dye, 83 Pt–Co of color, 33.7 NTU of turbidity, and 582 mg/L of COD were eliminated from the textile effluent. The removal efficiencies were approximately 90.3% for BB41 dye, 89.3% for color, 69.4% for turbidity, and 62.7% for COD. The initial levels of COD and Turbidity

| Isotherm models | | BB41 | EBT |
|---|---|---|---|
| Dubinin-Radushkevich (D-R) isotherm | intercept | 2.515 | 1.908 |
| | slope | −9.98E + 08 | −3.53E + 07 |
| | β ($mol^2/k^2 J^2$) | 9.98E + 08 | 3.53E + 07 |
| | E (KJ/mol) | 2.24E-05 | 1.19E-04 |
| | qm | 12.366 | 6.739 |
| | $R^2$ | 0.933 | 0.887 |
| Freundlich isotherm | Intercept | 2.216 | 0.934 |
| | slope | 0.896 | 0.439 |
| | $1/n_f$ | 0.896 | 0.439 |
| | $K_f$ | 9.169 | 2.544 |
| | $R^2$ | 0.985 | 0.935 |
| Langmuir isotherm | Intercept | 0.017 | 0.11 |
| | slope | 0.0914 | 0.314 |
| | $Q_{max}$ | 58.48 | 9.09 |
| | $K_L$ | 0.187 | 0.35 |
| | $R_L$ | 0.15 | 0.087 |
| | $R^2$ | 0.995 | 0.995 |
| Temkin isotherm | intercept | 9.478 | 2.426 |
| | slope | 5.298 | 1.943 |
| | $B_T$(J/mol) | 5.298 | 1.943 |
| | $K_T$ L/mg) | 5.983 | 3.485 |
| | $R^2$ | 0.921 | 0.970 |

**Table 3.** Adsorption isotherm model analysis for BB41 and EBT.

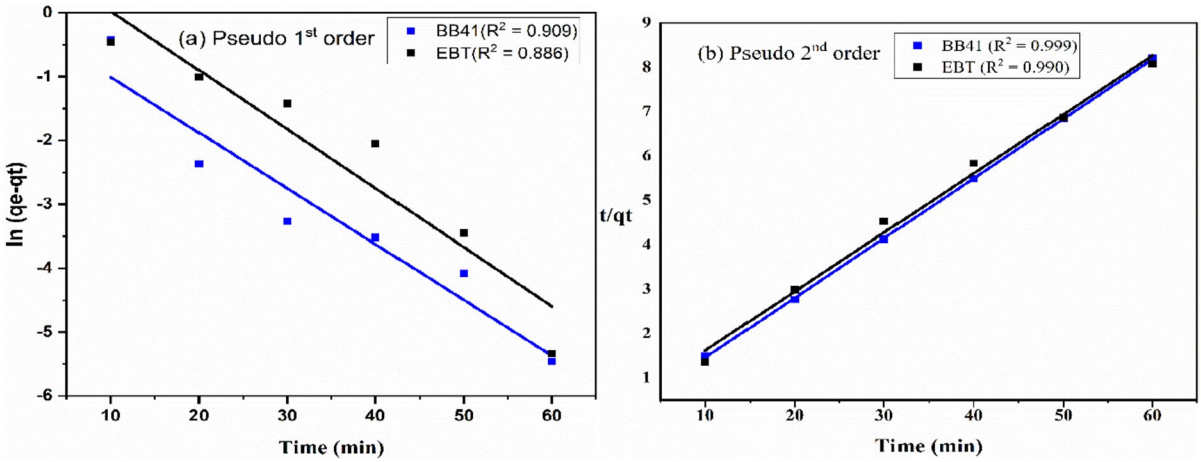


**Figure 12.** Adsorption kinetics model analysis graph (**a**) pseudo 1st order kinetics and(**b**) for pseudo 2nd order kinetics for BB41 and EBT dye.

| Kinetics models | dyes | intercept | slope | $q_e$ (mg/g) | $qe^2$ | $K_1$ | $K_2$ | $R^2$ |
|---|---|---|---|---|---|---|---|---|
| Pseudo 1st order | BB41 | -0.134 | −0.0872 | 0.874 | – | −0.00145 | – | 0.909 |
| | EBT | 1.592 | −0.0577 | 4.917 | – | −0.00096 | – | 0.886 |
| Pseudo 2nd order | BB41 | 0.0582 | 0.135 | 7.375 | 54.385 | – | 0.316 | 0.999 |
| | EBT | 1.259 | 0.148 | 6.734 | 45.346 | – | 0.0175 | 0.990 |

**Table 4.** Adsorption kinetics model analysis for BB41 and EBT dye.

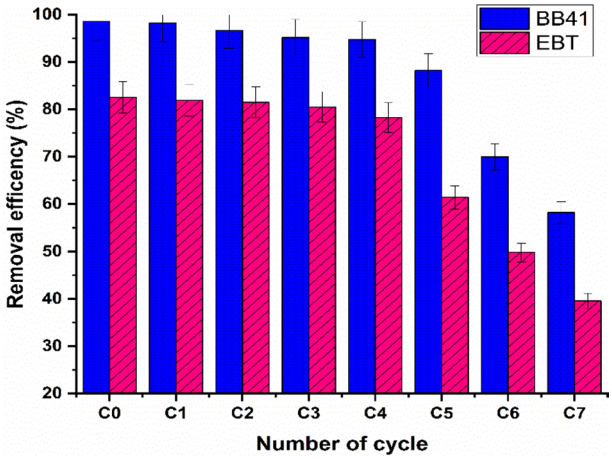


**Figure 13.** Removal of dyes under Giant reed BC of recycling test.

| Adsorbent | pollutants | Adsorption capacity | reference |
|---|---|---|---|
| rice husk BC | BB41 | 17.596 mg/g | [64] |
| Cocos Nucifera shell-derived BC | BB41 | 29.42 mg/g | [65] |
| pistachio shell adsorbent | BB41 | 41.77 mg/g | [60] |
| Giant reed BC | BB41 | 58.48 mg/g | This study |
| Waste hemp activated carbon (WHAC) | EBT | 14.025 mg/g | [66] |
| Giant reed BC | EBT | 9.06 mg/g | This study |

**Table 5.** Comparison of different BC adsorbents with removal adsorption capacity for BB41 and EBT dyes.

of the effluent influence the efficiency of the BC adsorbent. The adsorption process demonstrates good capacity in removing 582 mg COD within one hour, indicating its effectiveness. However, further treatment is required to meet the prescribed minimum threshold (< 5 NTU and < 250 mg/L) established by the IPA standard. A similar study also found a 76.0% COD removal of 611.04 mg/L using Teff straw BC [18]. This study demonstrates that BC exhibits strong adsorption capacity even at high levels of COD and Turbidity, providing further evidence of its effectiveness in removing harmful color pollutants from textile wastewater. Finally, the experience of studies is indicated in Table 5.

## Conclusions

The giant read BC adsorbent was successfully synthesized by slow pyrolysis techniques at 600 °C. This BC adsorbent showed excellent characteristics of a good adsorbent such as high fixed carbon (80.4%), low ash content (3.8%), large surface area (429 $m^2$/g), and excellent thermal stability. The BC exhibited notable adsorption capacity for both anionic and cationic azo dyes, as evidenced by the experimental findings. The results revealed a remarkable removal efficiency of 98.6% for BB41 dye and 82.5% for EBT dye were recorded. It was also found that the Langmuir isotherm model and pseudo-second-order kinetics provide the most suitable explanation for the adsorption of the two dyes onto the BC. This observation indicates that the adsorbent surface is uniform and monolayer and the adsorption mechanism is chemical. Furthermore, the BC was regenerated for up to four cycles while maintaining a performance degradation margin of 5% for both dyes. Further, it achieved 90.3% for BB41 dye, 89.2% for color, 69.4% for turbidity, and 62.7% for COD removal for real textile effluent. Therefore, giant reed BC adsorbent would be considered a new economical and environmentally friendly adsorbent for removing dye contaminants from the aqueous and which is also promising for the application of BC for wastewater remediation at large scale.

## Data availability

The datasets generated during and/or analysed during the current study are available from the corresponding author (Mohammednur Abdu, nuramsh@gmail.com) on reasonable request.

Received: 24 February 2024; Accepted: 18 July 2024
Published online: 07 August 2024

## References

1. Ahmed, S. & Ismail, S. Water pollution and its sources, effects & management: A case study of Delhi. International Journal of Current Advanced Research. **7**, 10436–10442 (2018).

2. Borah, D. K. & Bera, M. Watershed-scale hydrologic and nonpoint-source pollution models: Review of applications. *Trans. ASAE* **47**, 789 (2004).
3. Doetterl, S., Van Oost, K. & Six, J. Towards constraining the magnitude of global agricultural sediment and soil organic carbon fluxes. *Earth Surf. Process Landforms* **37**, 642–655 (2012).
4. Yadav, S., Chander, S., Gupta, A., Kataria, N. & Khoo, K. S. Biogenic engineered zinc oxide nanoparticle for sulfur black dye removal from contaminated wastewater: Comparative optimization, simulation modeling, and isotherms. *Bioengineered* **15**, 2325721 (2024).
5. Serejo, M. L. *et al.* Environmental Resilience by Microalgae. In *Microalgae Cultivation for Biofuels Production* (eds Serejo, M. L. *et al.*) (Elsevier, 2020).
6. Verma, A. K., Dash, R. R. & Bhunia, P. A review on chemical coagulation/flocculation technologies for removal of colour from textile wastewaters. *J. Environ. Manag.* **93**, 154–168 (2012).
7. Rose, P. K. *et al.* Congo red dye removal using modified banana leaves: Adsorption equilibrium, kinetics, and reusability analysis. *Groundw. Sustain. Dev.* **23**, 101005 (2023).
8. Mansour, R. Natural dyes and pigments: Extraction and applications. *Handbook. Renew. Mater. Color. Finish.* **9**, 75–102 (2018).
9. Salleh, M. A. M., Mahmoud, D. K., Karim, W. A. W. A. & Idris, A. Cationic and anionic dye adsorption by agricultural solid wastes: a comprehensive review. *Desalination* **280**, 1–13 (2011).
10. Hamdi, L., Boumehdi, L. & Salem, Z. Basic blue 41 dye removal from aqueous solution using lignocellulosic material: kinetics, equilibrium and statistical design optimization. *Int. J. Environ. Sci. Technol.* **20**, 3275–3294 (2023).
11. Kansal, S. K., Sood, S., Umar, A. & Mehta, S. K. Photocatalytic degradation of Eriochrome Black T dye using well-crystalline anatase TiO2 nanoparticles. *J. Alloys Compd.* **581**, 392–397 (2013).
12. Yaseen, D. A. & Scholz, M. Textile dye wastewater characteristics and constituents of synthetic effluents: a critical review. *Int. J. Environ. Tech.* **16**, 1193–1226 (2019).
13. Ai, L. *et al.* Removal of methylene blue from aqueous solution with magnetite loaded multi-wall carbon nanotube: Kinetic, isotherm and mechanism analysis. *J. Hazard. Mater.* **198**, 282–290 (2011).
14. Fazal, T. *et al.* Integrating adsorption and photocatalysis : A cost effective strategy for textile wastewater treatment using hybrid biochar-TiO 2 composite. *J. Hazard. Mater.* **390**, 121623 (2020).
15. Hutagalung, S. S., Muchlis, I. & Khotimah, K. Textile wastewater treatment using advanced oxidation process (AOP). In *IOP conference series: materials science and engineering* (ed. Hutagalung, S.) (IOP Publishing, 2020).
16. Samsami, S., Mohamadizaniani, M., Sarrafzadeh, M.-H., Rene, E. R. & Firoozbahr, M. Recent advances in the treatment of dye-containing wastewater from textile industries: Overview and perspectives. *Process Saf. Environ. Prot.* **143**, 138–163 (2020).
17. Yao, C., Wang, M., Jiang, W. & Chen, Y. %J E. E. R. Study on a novel N-doped mesoporous carbon for the efficient removal of methylene blue from aqueous solution. **26**, (2021).
18. Kifetew, M. *et al.* Adsorptive Removal of Reactive Yellow 145 Dye from Textile Industry Effluent Using Teff Straw Activated Carbon: Optimization Using Central Composite Design. *Water* **15**, 1281 (2023).
19. Rashid, R., Shafiq, I., Akhter, P., Iqbal, M. J. & Hussain, M. A state-of-the-art review on wastewater treatment techniques: the effectiveness of adsorption method. *Environ. Sci. Pollut. Res.* **28**, 9050–9066 (2021).
20. Fito, J. *et al.* Adsorption of methylene blue from textile industrial wastewater using activated carbon developed from Rumex abyssinicus plant. *Sci. Rep.* **13**, 5427 (2023).
21. Xiong, X. *et al.* A review of biochar-based catalysts for chemical synthesis, biofuel production, and pollution control. *Bioresourc. Technol.* **246**, 254–270 (2017).
22. Wang, W. *et al.* Preparation of TiO 2-modified Biochar and its Characteristics of Photo-catalysis Degradation for Enrofloxacin. Sci Rep. **10**, 1–12. https://doi.org/10.1038/s41598-020-62791-5 (2020).
23. Romanovski, V. Agricultural waste based-nanomaterials: Green technology for water purification. In *Aquananotechnology* (ed. Romanovski, V.) (Elsevier, 2021).
24. Lansdown, R. V, Knees, S. G. & Patzelt, A. Bacopa monnieri. The IUCN Red list of Threatened Species 2013. e. T164168A17722668. http://doi.org/10.2305/IUCN.UK.20131.RLTS.T164168A17722668.en (2013).
25. Ahmed, M. J. Potential of Arundo donax L. stems as renewable precursors for activated carbons and utilization for wastewater treatments. *J. Taiwan. Inst. Chem. Eng.* **63**, 336–343 (2016).
26. Zhao, Y., Huang, L. & Chen, Y. P. Biochars derived from giant reed (Arundo donax L.) with different treatment: characterization and ammonium adsorption potential. *Environ. Sci. Pollut. Res.* **24**, 25889–25898 (2017).
27. Eric, Y. Pb (II) removal from aqueous solution by biochar produced from giant reed. (2020).
28. Liu, G., Zheng, H., Zhai, X. & Wang, Z. Characteristics and mechanisms of microcystin-LR adsorption by giant reed-derived biochars: Role of minerals, pores, and functional groups. *J. Clean. Prod.* **176**, 463–473 (2018).
29. Hou, J., Huang, L., Yang, Z., Zhao, Y. & Deng, C. Adsorption of ammonium on biochar prepared from giant reed. *Environ. Sci. Pollut. Res.* https://doi.org/10.1007/s11356-016-7084-4 (2016).
30. Abewaa, M., Mengistu, A., Takele, T., Fito, J. & Nkambule, T. Adsorptive removal of malachite green dye from aqueous solution using Rumex abyssinicus derived activated carbon. *Sci. Rep.* **13**, 1–16 (2023).
31. Masuku, M., Nure, J. F., Atagana, H. I., Hlongwa, N. & Nkambule, T. T. I. Jo ur of. *Sci. Total Environ.* 168136 (2023) https://doi.org/10.1016/j.scitotenv.2023.168136.
32. Parsa, M., Nourani, M., Baghdadi, M., Hosseinzadeh, M. & Pejman, M. Biochars derived from marine macroalgae as a mesoporous by-product of hydrothermal liquefaction process: characterization and application in wastewater treatment. *J. Water Process Eng.* **32**, 100942 (2019).
33. Mohamed Noor, N., Shariff, A., Abdullah, N. & Aziz, S. Temperature effect on biochar properties from slow pyrolysis of coconut flesh waste. *Malaysian J. Fundam. Appl. Sci.* **15**, 153–158 (2019).
34. Maulina, S. & Iriansyah, M. Characteristics of activated carbon resulted from pyrolysis of the oil palm fronds powder. In *IOP conference series: materials science and engineering* (ed. Maulina, S.) (IOP Publishing, 2018).
35. Zhao, Y., Huang, L. & Chen, Y. Biochars derived from giant reed ( Arundo donax L.) with different treatment : characterization and ammonium adsorption potential. *Environ Sci. Pollut. Res.* https://doi.org/10.1007/s11356-017-0110-3 (2017).
36. Jedynak, K. & Charmas, B. Adsorption properties of biochars obtained by KOH activation. *Adsorption* https://doi.org/10.1007/s10450-023-00399-7 (2023).
37. Guilhen, S. N. *et al.* Role of point of zero charge in the adsorption of cationic textile dye on standard biochars from aqueous solutions. *Recent Prog. Mater.* **4**, 1–30 (2022).
38. Jindo, K., Mizumoto, H., Sawada, Y., Sanchez-Monedero, M. A. & Sonoki, T. Physical and chemical characterization of biochars derived from different agricultural residues. *Biogeosciences* **11**, 6613–6621 (2014).
39. Tan, X. *et al.* Application of biochar for the removal of pollutants from aqueous solutions. *Chemosphere* **125**, 70–85 (2015).
40. Yan, Y., Manickam, S., Lester, E., Wu, T. & Pang, C. H. Synthesis of Graphene Oxide and Graphene Quantum Dots from Miscanthus via Ultrasound-Assisted Mechano-Chemical Cracking Method. *Ultrason. Sonochem.* **73**, 105519 (2021).
41. Tam, N. T. M. *et al.* Synthesis of porous biochar containing graphitic carbon derived from lignin content of forestry biomass and its application for the removal of diclofenac sodium from aqueous solution. *Front. Chem.* **8**, 274 (2020).
42. Galashev, A. & Rakhmanova, O. Mechanical and thermal stability of graphene and graphene-based materials. *Physics-Uspekhi* **57**, 970–989 (2014).

43. Hadey, C., Allouch, M., Alami, M., Boukhlifi, F. & Loulidi, I. Preparation and Characterization of Biochars Obtained from Biomasses for Combustible Briquette Applications. *Sci. World J.* **2022**, 2554475 (2022).
44. Le, P. T. *et al.* Preparation and Characterization of Biochar Derived from Agricultural By-Products for Dye Removal. *Adsorpt. Sci. Technol.* 1–14. https://doi.org/10.1155/2021/9161904 (2021).
45. Arwenyo, B., Navarathna, C., Das, N. K., Hitt, A. & Mlsna, T. Sorption of Phosphate on Douglas Fir Biochar Treated with Magnesium Chloride and Potassium Hydroxide for Soil Amendments. *Processes* **11**, 331 (2023).
46. Md Salim, R., Asik, J. & Sarjadi, M. S. Chemical functional groups of extractives, cellulose and lignin extracted from native Leucaena leucocephala bark. *Wood Sci. Technol.* **55**, 295–313 (2021).
47. Yeboah, M. L., Li, X. & Zhou, S. Facile Fabrication of Biochar from Palm Kernel Shell Waste and Its Novel Application to Magnesium-Based Materials for Hydrogen Storage. *Materials* **13**, 625 (2020).
48. Patel, S. *et al.* Production of H2 and CNM from biogas decomposition using biosolids-derived biochar and the application of the CNM-coated biochar for PFAS adsorption. *Waste Manag.* **159**, 146–153 (2023).
49. Dervishi, E., Ji, Z., Htoon, H., Sykora, M. & Doorn, S. K. Raman spectroscopy of bottom-up synthesized graphene quantum dots: Size and structure dependence. *Nanoscale* **11**, 16571–16581 (2019).
50. Zhang, Z. *et al.* Development of iron-based biochar for enhancing nitrate adsorption: Effects of specific surface area, electrostatic force, and functional groups. *Sci. Total Environ.* **856**, 159037 (2023).
51. Amen, R. *et al.* Lead and cadmium removal from wastewater using eco-friendly biochar adsorbent derived from rice husk, wheat straw, and corncob. *Clean. Eng. Technol.* **1**, 100006 (2020).
52. Nasir, M., Rahmawati, T. & Dara, F. Synthesis and Characterization of Biochar from Crab Shell by Pyrolysis. *IOP Conf. Ser. Mater. Sci. Eng.* **553**, 12031 (2019).
53. Salman, S. *et al.* Improving copper ( II ) ion detection and adsorption from wastewater by the ligand-functionalized composite adsorbent. *J. Mol. Struct.* **1282**, 135259 (2023).
54. Praveen, S., Jegan, J., Bhagavathi, T. & Ravindiran, P. Biochar for removal of dyes in contaminated water : an overview. *Biochar* https://doi.org/10.1007/s42773-022-00131-8 (2022).
55. Dugmore, T., Bansal, M. & Patnala, P. Adsorption of Eriochrome Black-T(EBT) using tea waste as a low cost adsorbent by batch studies: A green approach for dye effluent treatments. *Curr. Res. Green Sustain. Chem.* **3**, 100036 (2020).
56. Li, D., Yan, J., Liu, Z. & Liu, Z. Adsorption kinetic studies for removal of methylene blue using activated carbon prepared from sugar beet pulp. *Int. J. Environ. Sci. Technol.* **13**, 1815–1822 (2016).
57. Oetjik, W. & Ibrahim, S. A. A review: the effect of initial Dye concentration and contact time on the process of Dye adsorption using agricultural wastes adsorbent. *Prog. Eng. Appl. Technol.* **2**, 1051–1059 (2021).
58. El-Sayed, G. O., Yehia, M. M. & Asaad, A. A. Assessment of activated carbon prepared from corncob by chemical activation with phosphoric acid. *Water Resour. Ind.* **7–8**, 66–75 (2014).
59. Xiong, S. *et al.* Adsorption isotherm and equilibrium process of dye wastewater onto camphor sawdust. *Nat. Environ. Pollut. Technol.* **15**, 689 (2016).
60. Alzein, M. Adsorptive removal of basic blue 41 using pistachio shell adsorbent - Performance in batch and column system. *Sustain. Chem. Pharm.* **16**, 100254 (2020).
61. Nizam, N. U. M., Hanafiah, M. M., Mahmoudi, E., Halim, A. A. & Mohammad, A. W. The removal of anionic and cationic dyes from an aqueous solution using biomass-based activated carbon. *Sci. Rep.* **11**, 8623 (2021).
62. Thillainayagam, B. P. & Nagalingam, R. Batch and column studies on removal of eriochrome black T dye by microalgae biochar. *Glob. NEST J.* **25**, 6–16 (2023).
63. Cheung, P. C. W. *et al.* Decolourisation of Metal-azo Dyes in Wastewaters by Sodium Peroxodisulphate : A Template for Experimental Investigations. *Open Environ. Res. J.* https://doi.org/10.2174/25902776-v16-e230216-2022-2 (2023).
64. Saravanan, P. & Josephraj, J. Evaluation of the adsorptive removal of cationic dyes by greening biochar derived from agricultural bio-waste of rice husk. 4047–4060 (2023).
65. Saravanan, P., Thillainayagam, B. P., Ravindiran, G. & Josephraj, J. Evaluation of the adsorption capacity of Cocos Nucifera shell derived biochar for basic dyes sequestration from aqueous solution. *Energ. Sourc. Part A: Recover. Utilizat. Environ. Effect.* 1–17. https://doi.org/10.1080/15567036.2020.180014266 (2020)
66. El Mansouri, F. *et al.* Efficient Removal of Eriochrome Black T Dye Using Activated Carbon of Waste Hemp (Cannabis sativa L.) Grown in Northern Morocco Enhanced by New Mathematical Models. *Separations* **9**, 283 (2022).


## Acknowledgements

The authors thank Addis Ababa Science and Technology University for financial support and Environmental Engineering Department for laboratory services. The authors thank Wollo University and KiOT for financial support.

## Author contributions

All authors have contributed to this paper, the concept development (M A and J N), draft preparation and revision (M.A, SB, JN, TM), and approved submission (MA, AW, SB, JN, TM).

## Funding

This research was funded by the Addis Ababa Science and Technology University (AASTU).

## Competing interests

The authors declare no competing interests.

## Additional information

**Correspondence** and requests for materials should be addressed to M.A.

**Reprints and permissions information** is available at www.nature.com/reprints.

**Publisher's note** Springer Nature remains neutral with regard to jurisdictional claims in published maps and institutional affiliations.



**Open Access** This article is licensed under a Creative Commons Attribution-NonCommercial-NoDerivatives 4.0 International License, which permits any non-commercial use, sharing, distribution and reproduction in any medium or format, as long as you give appropriate credit to the original author(s) and the source, provide a link to the Creative Commons licence, and indicate if you modified the licensed material. You do not have permission under this licence to share adapted material derived from this article or parts of it. The images or other third party material in this article are included in the article's Creative Commons licence, unless indicated otherwise in a credit line to the material. If material is not included in the article's Creative Commons licence and your intended use is not permitted by statutory regulation or exceeds the permitted use, you will need to obtain permission directly from the copyright holder. To view a copy of this licence, visit http://creativecommons.org/licenses/by-nc-nd/4.0/.

© The Author(s) 2024